Biosensors and Bioelectronics xx (xxxx) xxxx–xxxx

Contents lists available at ScienceDirect

Biosensors and Bioelectronics

journal homepage: www.elsevier.com/locate/bios

Rapid fluorometric bacteria detection assay and photothermal effect by fluorescent polymer of coated surfaces and aqueous state

Zihnil Adha Islamy Mazrad[a], Insik In[a,b], Kang-Dae Lee[c,*], Sung Young Park[a,d,**]

[a] Department of IT Convergence, Korea National University of Transportation, Chungju 380-702, Republic of Korea
[b] Department of Polymer Science and Engineering, Korea National University of Transportation, Chungju 380-702, Republic of Korea
[c] Department of Otolaryngology-Head and Neck Surgery, Kosin University College of Medicine, Busan 49267, Republic of Korea
[d] Department of Chemical and Biological Engineering, Korea National University of Transportation, Chungju 380-702, Republic of Korea

ARTICLE INFO

Keywords:
Fluorescent polymer
Quenching
Bacteria detection
Photothermal effect
Coated surface

ABSTRACT

A fluorescent dye and a photothermal agent were grafted onto a cationic polymer for rapid and simple bacteria detection in liquid and solid phase based fluorescence on/off. The integrated poly(vinylpyrrolidone) (PVP) backbone with catechol and bromoethane moieties possesses unique optical properties due to the presence of boron dipyrromethane (BODIPY) and near infared NIR-responsive IR825 (F-PVP). The cationic segments showed distinct fluorescence quenching patterns after interaction with gram-positive and gram-negative bacteria via polyion complex interactions. Fluorescence quenching depended on direct interaction of the bacterial cell membrane, as confirmed using SEM and confocal imaging. The detection limit was 1 mg/mL for the liquid-phase assay and the minimal detectable concentration of bacteria using the solid-phase assay was 10^6 CFU/mL. After bacterial detection in contaminated area, our system can directly kill bacteria via the photothermal conversion ability of the IR825 substituent using NIR exposure by polymer solution and limited in coated PP. Finally, the proposed biosensor is capable as potential material for detection of bacteria in simple liquid and solid phase assay.

1. Introduction

Bacterial contamination in medical devices is a major public health concern, which has attracted global attention, as it can cause fatal diseases, resulting in an increased death rate of patients and increased medical costs (Fauci and Morens, 2012; Kang et al., 2014; Khan et al., 2009). Various techniques have been used to detect microbial infections, including specimen culturing, polymerase chain reaction (PCR), and target-specific immunoassays (Lazcka et al., 2007; Valloran et al., 2016; Wang et al., 2015). PCR is the most commonly used method due to its efficiency and specificity, but it requires sophisticated instruments and costly dye-labeled primers for whole step detection (Gebert et al., 2008; Wilson et al., 1995). Fluorescent quantum dots have been reported to be useful for sensing of multiple pathogens through antibody conjugation. However, challenges remain for fluorescence-based detection; the major problem is development of a method for large-scale and reproducibility of quantum dots (QDs) with thin, biocompatible coatings (Ray et al., 2012; Zhao et al., 2009). Therefore, further research is required to develop rapid, simple, and inexpensive methods for responsive bacterial detection.

Considering interaction mechanism between cell and material, which are many groups in bacterial cell outer membranes, which can be deprotonated to produce negative charges, there may be many ways to improve current techniques. We therefore attempted to develop an advanced method for bacterial detection by exploiting the negative charge on bacteria. Cationic conjugated polymers are a promising platform to interact with the negative charge on the surface of bacteria without extensive biochemical preparation, understanding single electrostatic interaction can be used to design a simple and rapid detection technique (Bandyopadhyay et al., 2015; Miranda et al., 2011; Wilson et al., 2001). A few reports have discussed bacterial detection based on fluorescence on/off system. Cationic poly(phenylene vinylene) polymers have been reported to be effective for detection and discrimination of single bacteria in aqueous media based on the intensity of the fluorescence signal; polyion complex micellar nanoparticles showed fluorescence quenching after competitive binding with bacteria, and aggregation of the cationic CdTe QDs on the surface of bacteria was reported to result in quenching of the fluorescence of the CdTe QDs (Y.Q. Li et al., 2014; Y. Li et al., 2014; Yang et al., 2015; Yuan et al., 2014). Along these examples, the interaction between negatively

* Corresponding author.
** Corresponding author at: Department of IT Convergence, Korea National University of Transportation, Chungju 380-702, Republic of Korea.
E-mail addresses: kdlee59@gmail.com (K.-D. Lee), parkchem@ut.ac.kr (S.Y. Park).

http://dx.doi.org/10.1016/j.bios.2016.10.027
Received 30 August 2016; Received in revised form 10 October 2016; Accepted 13 October 2016
Available online xxxx
0956-5663/

charged bacteria and synthetic material–based fluorescence quenching generated different patterns for gram-negative and gram-positive bacteria; most of the gram-positive bacteria showed only a slight quenching effect, owing to the difficulty of the chemical interaction between the negative charges in the long chain technoic acid with the positively charged bacterial surface (Birdsell et al., 1975). A recent work, reported only a limited capacity for bacterial detection in aqueous phase and no reports have been published on emission-based bacterial detection in solid phase assay (Chen et al., 2014; Chung et al., 2013; Y.Q. Li et al., 2014; Y. Li et al., 2014; Ning et al., 2011). The aim of the present work was to design a polymer for both detection and killing of bacteria, not only in solution but also in a solid-phase assay. This proposed system offers a novel, simple, and rapid method for detection of bacteria.

The developed materials were prepared using Boron dipyrromethane (BODIPY) dye and IR825 conjugated to poly(vinylpyrrolidone) (PVP) using a quarternization method and the cationic moieties were obtained from excess conjugated bromoethane in the polymer system. For solid detection, the catechol moieties were used to fabricate adhesive properties so that it can be applied to propylene (PP) films. The combined polymer, with positively charged amine groups, possesses the tunable fluorescence of BODIPY and the excellent heat conversion of near infrared (NIR)-responsive IR825. The interaction of the prepared polymer with bacteria was expected to result in fluorescence quenching, for use in bacterial detection. Coating of PP films with the prepared polymer produced a detection pattern similar to that observed in liquid media, confirming that the material shows promise for use in biosensors in the fields of microbiology and medicine. After detection, this biosensor can directly kill bacteria using the photothermal conversion ability of the IR825 substituent. This platform shows excellent potential for development of materials that can detect bacteria within a second, followed by direct killing of bacteria.

2. Material and methods

2.1. Materials and characterization

Poly(vinylpyrrolidone) (PVP, 40,000 MW), 2-chloro-3′,4′-dihydroxyacetophenone (CCDP), bromoethane ethanol, nitrogen, deionized water, phosphate-buffer saline (PBS), diethyl ether, MRS, lysogeny broth (LB), deuterium oxide (D_2O), dimethyl sulfoxide (DMSO), propylene (PP), 3-(4,5-dimethylthiazol-2-yl)-2,5-diphenyltetrazolium bromide (MTT), and agar were purchased from Sigma-Aldrich, Yongin City, Kyunggi-Do, South Korea. Propidium iodide and SYTO 9 were purchased from Molecular Probe, Life Technologies (Invitrogen). Boron dipyrromethane (BODIPY) with benzyl chloride on the meso position was prepared as previously described, and the heptamethine dye IR825 was synthesized using a previously reported protocol (Chae and Baek, 2012; Cheng et al., 2013).

^{1}H NMR spectra was recorded using (Bruker AVANCE 400 spectrometer operating at 400 MHz) with DMSO as the solvent. The absorption spectra of the sample were recorded using a UV–vis absorption spectrometer (UV–vis, Optizen 2120 UV spectrophotometer, Mecasys, Yuseong-gu Daejeon, South Korea). The fluorescent properties were measured using a L550B luminescence spectrometer from Perkin Elmer. The NIR laser was set at 808 nm (PSU-III-LRD, CNI Optoelectronics Tech. Co. LTD, China). Photothermal heating curves were examined using an infrared camera (NEC Avio, Thermo Tracer TH9100). Field-emission scanning electron microscopy (FE-SEM) micrographs were obtained using a SEM/EDX, JSM-6700F, JEOL, Musashino, Akishima, Tokyo, Japan. X-ray photoelectron spectra (XPS) were acquired using an ESCALAB apparatus (Omicrometer, Taunusstein, Germany) and a system (PHI Quantera-II, Ulvac-PHI, Chigasaki, Kanagawa, Japan). Live/dead bacterial analysis was performed using a LSM510 confocal laser scanning microscope (CLSM, Carl Zeiss, Germany) using 405, 488, and 543 nm emission filters with 20× magnification. Particle size was measured with dynamic light scattering (DLS; Zetasizer Nano, Malvern-Germany). Static water contact angles were measured with a DO3210 instrument (KRUSS Ltd., Germany).

2.2. Synthesis of CCDP/IR825/BODIPY/ethyl bromide quaternized PVP (F-PVP)

The CCDP/IR825/BODIPY/ethyl bromide–conjugated PVP was synthesized using the quaternization reaction as previously described (Kang et al., 2016). In detail, PVP (2 g) and CCDP (0.3032 g) were dissolved in 60 mL of anhydrous ethanol in a 250-mL then stirred for 12 h at 70 °C under a nitrogen atmosphere. At the end of the reaction, solvent was evaporated and precipitated using diethyl ether. The resulting CCDP quaternized PVP (C-PVP) was dried in a vacuum oven and used for the next step. The BODIPY (0.0746 g), IR825 (0.3 g) and an excess of bromoethane (1.12 mL) as cationic moieties were quaternized with C-PVP (4 g) using the same method above but conducted for 48 h under a nitrogen atmosphere. Un-reacted precursors were removed on a rotary evaporator then precipitated using diethyl ether, and the residues were processed in a vacuum oven to obtain a dried sample.

The conjugated polymer was characterized using ^{1}H NMR spectroscopy (Fig. 1). ^{1}H NMR (400 MHz, d6-DMSO, δ): 0.81–1.25 (2H, $-CH_2$ of PVP), 2.12–2.23 (2H, $-CH_2$ of VP ring), 2.24–2.32 (2H, $-CH_2$ of VP ring), 3.15–3.28 (2H, $-CH_2$ of VP ring), 3.47–3.66 (H, –CH of PVP), 6.67–7.53 (aromatic protons of catechol), 0.94 (3H, $-CH_3$–CH_2 of BODIPY), 1,3 (3H, $-CH_3$ of BODIPY), and 7.9–8.3 (2H, aromatic proton of BODIPY and IR825).

2.3. Preparation of coated PP

PP-coated F-PVP was obtained using a dip-coating method, using catechol chemistry in PBS (pH 8.5) (Lee et al., 2008). PP film were cut into small pieces (5 cm) and rinsed with ethanol and deionized water followed dried using dryer pump. These PP slides were immersed in a F-PVP solution (10 mg/mL, PBS pH 8.5) for 24 h and then dried in air. In the end, we named this treated PP as coated PP.

2.4. The liquid and solid-phase detection assay using F-PVP with bacteria

For liquid-phase detection assay, the solutions of *S. aureus* (gram-positive, strain ATCC 25323) and *E. coli* (gram-negative, strain ATCC 25922) were prepared in LB and MRS broth (50 mL) media, respectively, and incubated at 37 °C for 24 h. Then F-PVP solution (1 mg/mL) was added to the bacterial solution (10^8 cells/mL) and incubated for 1 h. At the end of incubation period, the solution was centrifuged followed by washing with PBS to remove the unreacted F-PVP. To verify the capacity of the F-PVP for detection of single bacteria, the bacterial pellet labeled with F-PVP was added with PBS (pH 7.4) solution and then the fluorescent properties were observed using a L550B luminescence spectrometer at an excitation wavelength of 520 nm and a LSM510 confocal laser scanning microscope (Scheme S1a).

For solid-phase detection assay, the coated PP was added to solutions of each bacterial strain at a concentration of 10^8 cells/ mL and incubated for 1 h. After the incubation period, the coated PP was removed from the bacterial solution and washed with PBS. The coated PP was dried at room temperature and its fluorescent properties were measured using a LSM510 confocal laser scanning microscope as illustrated in Scheme S1b.

2.5. Scanning electron microscopy for bacterial cell imaging

For SEM imaging, the bacterial suspensions obtained using similar

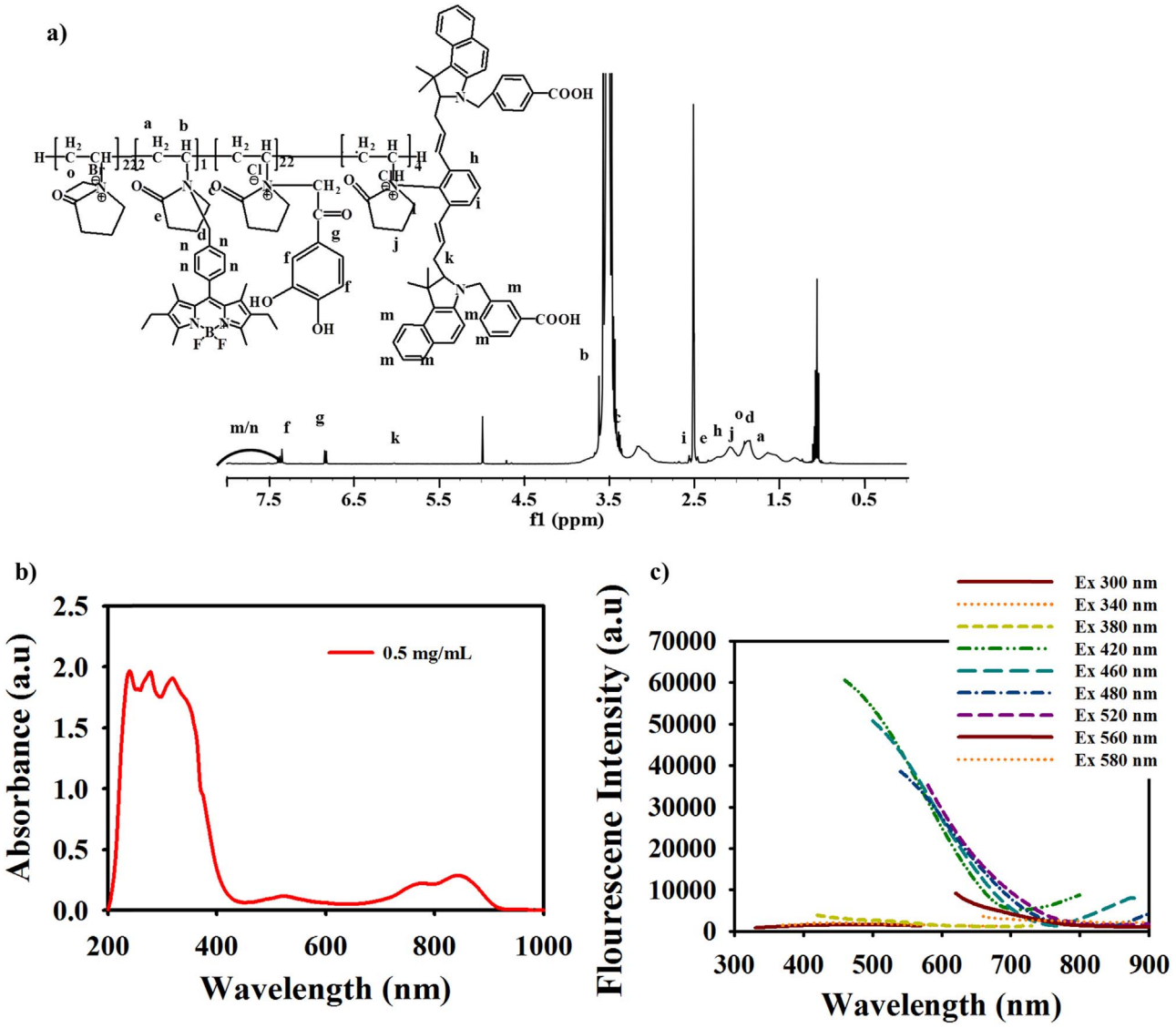

Fig. 1. (a) ^{1}H NMR spectra of F-PVP. (b) UV–vis spectrum of F-PVP. (c) Corresponding emission spectra of F-PVP with different excitation at a concentration of 5 mg/mL in water.

method with bacteria detection assay were centrifuged followed by washing with ethanol (25%, 50%, 75%, and 99%) consecutively (Fischer et al., 2012). A few microliters of the untreated and treated bacteria were then dropped on a silicon wafer and incubated for 3–4 h for drying. The dried treated bacteria on the silicon wafers were used to record SEM micrographs. F-PVP-coated PP treated with solutions of *S. aureus* and *E. coli* were prepared using method shown in Scheme S1b. After washing with PBS, the coated PP was dried at room temperature and then the interaction of bacterial cells with coated PP was observed using FE-SEM.

2.6. Live/dead bacterial assay

Bacteria labeled with F-PVP were centrifuged (4000 rpm for 5 min) and re-suspended in PBS solution. Then, 5 µL of the bacterial suspension was mixed with 20 µL of a fluorescent probe mixture containing 3.0 µm green fluorescent nucleic acid stain SYTO 9 (Invitrogen, USA) and 15.0 µm red fluorescent nucleic acid stain PI (Sigma-Aldrich, USA). The F-PVP (1 mg) was incubated with 1 mL of bacterial suspension of both *S. aureus* and *E. coli* (10^5 cells/mL) in a 2-mL EP tube at 2 W/m^2 for 5 min (808 nm laser). The 5-µL aliquot was incubated in the dark for 15 min then placed on a glass slide, which was then covered with a cover slip, sealed, and examined under an LSM510 confocal laser scanning microscope (Carl Zeiss, Germany) equipped with a He Ne laser at 488, and 543 nm. The above method was followed for fluorescence cell imaging. Furthermore, we investigated bacteria killing efficiency of F-PVP at concentration from 10^2 to 10^8 cells/mL under NIR irradiation along the 3-(4,5-dimethylthiazol-2-yl)-2,5-diphenyltetrazolium bromide (MTT) assay. The S. *aureus* and E. *coli* cells were incubated with F-PVP for 1 h then irradiated with NIR laser for 5 min. The treated cells were washed with PBS pH 7.4 and centrifuged to remove cells medium. A total of 20 µL of a stock solution containing 15 mg of MTT in 3 mL of PBS was added and incubated for an additional 4 h. Finally, 180 µL of MTT-solubilizing agent was added to the cells, which were shaken for 15 min. The absorbance was measured at a wavelength of 570 nm using microplate reader (Varioskan Flash, Thermo Electron Corporation) Relative cell viability was evaluated by comparison with the control well, which contained the cells without NIR irradiation.

3. Results and discussion

3.1. Formation of combined polymer for dual-phase detection of bacteria

The negative charge of the bacterial surface offers an excellent

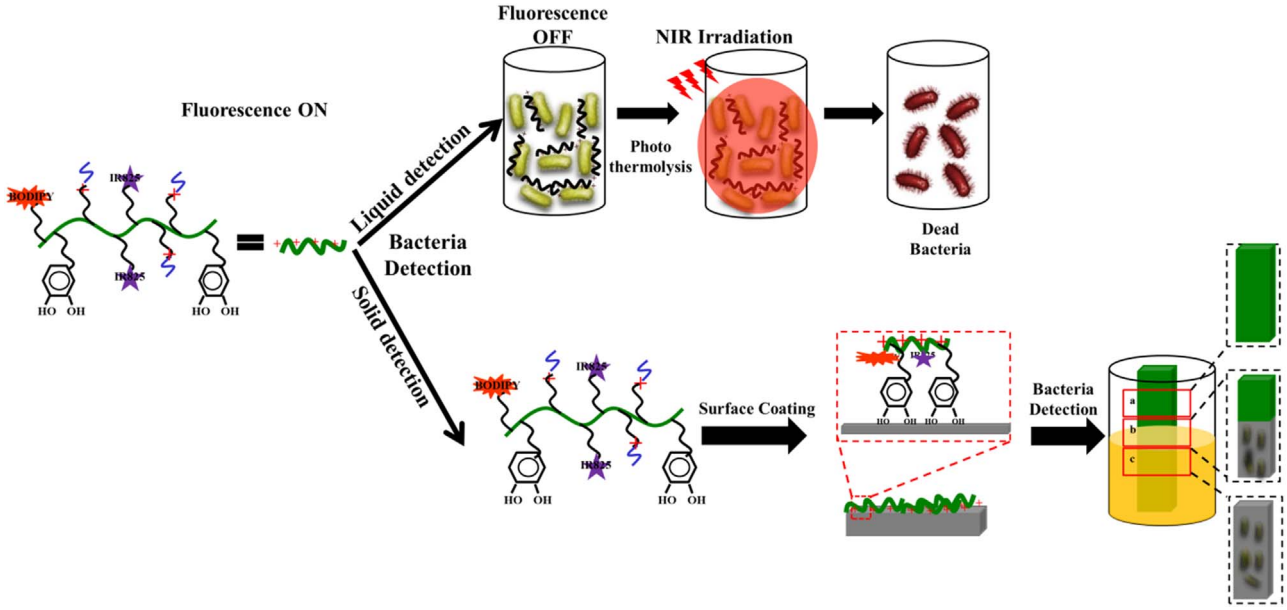

Scheme 1. Illustration of the preparation and application of F-PVP for liquid and solid-phase bacterial detection assay.

opportunity for design of a new platform for bacterial detection based on an understanding of the interaction between the materials and the negatively charged bacteria. In this study, we designed a promising polymer for detection and thermal killing of microbes, combining the fluorescent dye BODIPY; sufficient photothermal generation was ensured by integrating IR825 within the PVP polymer backbone. The bromoethane substituent was quaternized to the prepared polymer to obtain cationic charges. To further improve detection, the adhesive catechol moieties integrated into this design through quarternization were used for coating surfaces such as PP (Lee et al., 2008). Scheme 1 illustrates the technique for dual-phase detection of bacteria, in liquid- and solid-phase assays. The combined polymer showed fluorescent properties, and after interacting with bacteria in liquid medium, the fluorescence was quenched. Meanwhile, the NIR-responsive IR825 released heat, and had an antibacterial effect on both gram-positive and gram-negative strains (Park et al., 2016). A unique feature of our detection technique is the capacity for use in a solid assay; by utilizing the adhesive catechol chemistry, this system can be used to coat many types of surfaces, exhibiting a similar pattern for detection of bacteria based on fluorescence intensity.

3.2. Material characterization

The chemical structure of the integrated BODIPY, IR825, CCDP, and bromoethane in PVP polymer was demonstrated by the ^{1}H NMR and UV–vis spectra. The ^{1}H NMR spectra generated an aromatic proton peak at 7.5–8.5 ppm, corresponding to the presence of BODIPY and IR825 species in the PVP polymer composite; the intense peak at 1.6–2 ppm reflected the ethyl substituent in the polymer backbone (Fig. 1a). Cationic F-PVP shows good solubility in water due to the presence of the quaternized amine terminal group, as shown in Fig. S2. Moreover, investigation of the optical properties of F-PVP in water using UV–vis–NIR spectroscopy showed the presence of a catechol group at 250–300 nm, indicating π–π^* electron transitions in phenolic compounds, and the intense peaks at 550 nm and 800 nm confirmed the presence of BODIPY and IR825 in the polymer backbone, respectively (Cheng et al., 2013; S.Y. Lee et al., 2014; K.S. Lee et al., 2014). The absorption peak of F-PVP demonstrates the presence of potential photothermal agents responsive to NIR irradiation in the range ~650 to 900 nm (Fig. 1b) (Cho et al., 2015). Therefore, the capacity for heat generation followed NIR light exposure was examined at various concentrations in aqueous solution. As shown in Fig. S4, the thermal elevation curve displays a sharp increase in heat release with increasing concentration. The BODIPY dye in the cationic polymer takeover produced strong green fluorescence, a prominent feature of F-PVP. Fig. 1c shows that F-PVP possesses excitation-dependent fluorescence emission band at 450–650 nm when excited at 520 nm (Kang et al., 2016).

3.3. Bacteria detection in liquid phase

Interactions between the chemical structure of the bacterial cell wall and F-PVP have been investigated using photoluminescence spectroscopy, for potential use as fluorescence on/off detection method (Fig. 2a and b). The fluorescence intensity of different concentrations F-PVP was quenched after incubation with both bacterial strains, *E. coli* and *S. aureus,* compared with the emission intensity at a concentration of 5 mg/mL in water. The significant quenching effect of *E. coli* at all concentrations of F-PVP was due to a strong electrostatic interaction, whereas the dominant hydrophobic interaction than ionic complex in the *S. aureus* cell wall meant that a maximal F-PVP concentration of 1 mg/mL resulted in fluorescence quenching (Yuan et al., 2014). Phosphate groups and phospholipids spread in whole surface *E. coli* that easily form electrostatic bonds, resulting in fluorescence quenching of F-PVP due to formation of ionic complexes with the bacteria. In contrast to *E. coli*, the negative charges on S. *aureus* is located in the long chain of teichoic acid exposed on the cell surface, reflecting the dominance of hydrophobic interactions, so that generated lesser quenching effect than *E. coli* (Birdsell et al., 1975; Jann et al., 1975). As shown in Fig. S3a and b, CLSM images of bacteria labeled with F-PVP showed fluorescence quenching for both bacterial strains, confirming that F-PVP can detect bacteria at low concentrations in water. Fig. S3a (*S. aureus* labeled with F-PVP at 10 mg/L) showed bright green fluorescence, concordant with the PL spectra of *S. aureus* (Fig. 2b) treated with F-PVP at 10 mg/mL, reflecting the limited detection capacity at high concentrations for gram-positive bacteria.

To evaluate the direct interaction of F-PVP and bacteria, 1 mg/mL of F-PVP was added to both types of bacteria and monitored using imaging. The smooth bacterial surface was visibly different after interaction with F-PVP, because the F-PVP adhered to the surface of the bacteria could be seen, reflecting F-PVP binding with bacteria (Fig. 2c and d). For further evidence of the direct interaction between

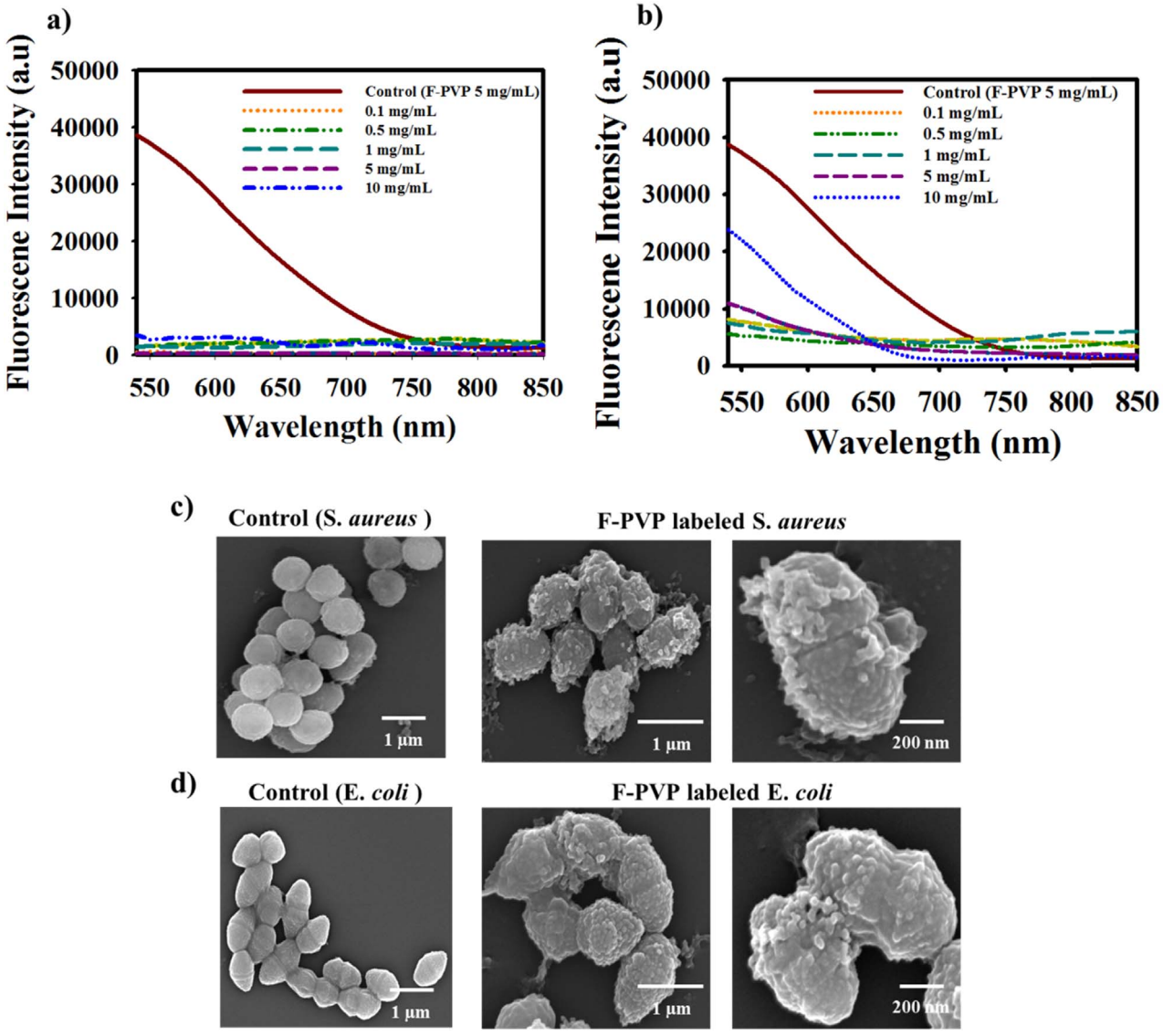

Fig. 2. Detection of bacteria in liquid medium at varying concentrations of F-PVP using fluorescence emission intensity. PL spectra of (a) *E. coli* labeled with F-PVP (b) *S. aureus* labeled with F-PVP. FE-SEM images of (c) *S. aureus*, *S. aureus* labeled with F-PVP and single *S. aureus* labeled with F-PVP (d) *E. Coli E. coli* labeled with F-PVP and single *E. coli* labeled with F-PVP. The bacterial concentration was 10^8 CFU/mL and the concentration of F-PVP was 1 mg/mL for SEM imaging.

the bacteria and F-PVP, dynamic light scattering was used to investigate the size of treated bacteria in water. The particle size of *E. coli* and *S. aureus* labeled with F-PVP was observed rise from 1206.6 nm and 1060.567 nm to be 1308 nm and 1154 nm, respectively (Fig. S6). The increase in size indicates the interaction between the bacteria and F-PVP.

3.4. Solid phase detection performance

Surface-accessible catechol and its derivatives are widely used in the fabrication of a broad range for coating agents in various substrates (Wei et al., 2014; Yeroslavsky et al., 2015). As can be seen in Fig. S8, the application of F-PVP on PP surfaces using a dip-coating method revealed a decrease in hydrophobicity, as shown by the reduction in water contact angle (Kim et al., 2016; S.Y. Lee et al., 2014; K.S. Lee et al., 2014; Magin et al., 2010).

The fluorescence on/off design was further checked against F-PVP in PP substrates, new concept based detection in solid phase assay. F-PVP coated on a PP surface emits green fluorescence under a laser scanning microscope. These results revealed promising potentiality to draw fluorescence image on versatile substrates. We tested the performance of coated PP in bacterial solutions at three points (top, middle, and bottom) in order to determine the fluorescence quenching response. As shown in Fig. 3, the observed light emission was noticeably decreased at the bottom, where there was a strong interaction between the negatively charged bacterial surfaces with the positive charges generated as a consequence of quaternization of the amino groups of F-PVP (Goy et al., 2016). A polyionic complex interaction occurred between the bacteria and the positively charged F-PVP on the surface of the PP, resulting in fluorescence quenching, indicating the presence of bacteria (Y.Q. Li et al., 2014; Y. Li et al., 2014). These results indicate that F-PVP applied on a PP surface shows promise for simple and easy detection of bacteria within a single second, based on color changes. We extended our study to determine the sensitivity for detection of bacteria dependent on the concentration. Coated PP was able to detect both types of bacteria at a minimum concentration of 10^6 cells/mL; concentrations below 10^6 CFU/mL still yielded a strong fluorescent signal in comparison to high bacterial concentrations, as seen in Fig. 3b and c. As the concentration of bacteria decreased, a decreasing number of bacterial interactions with the coated PP were generated, causing a reduced quenching effect.

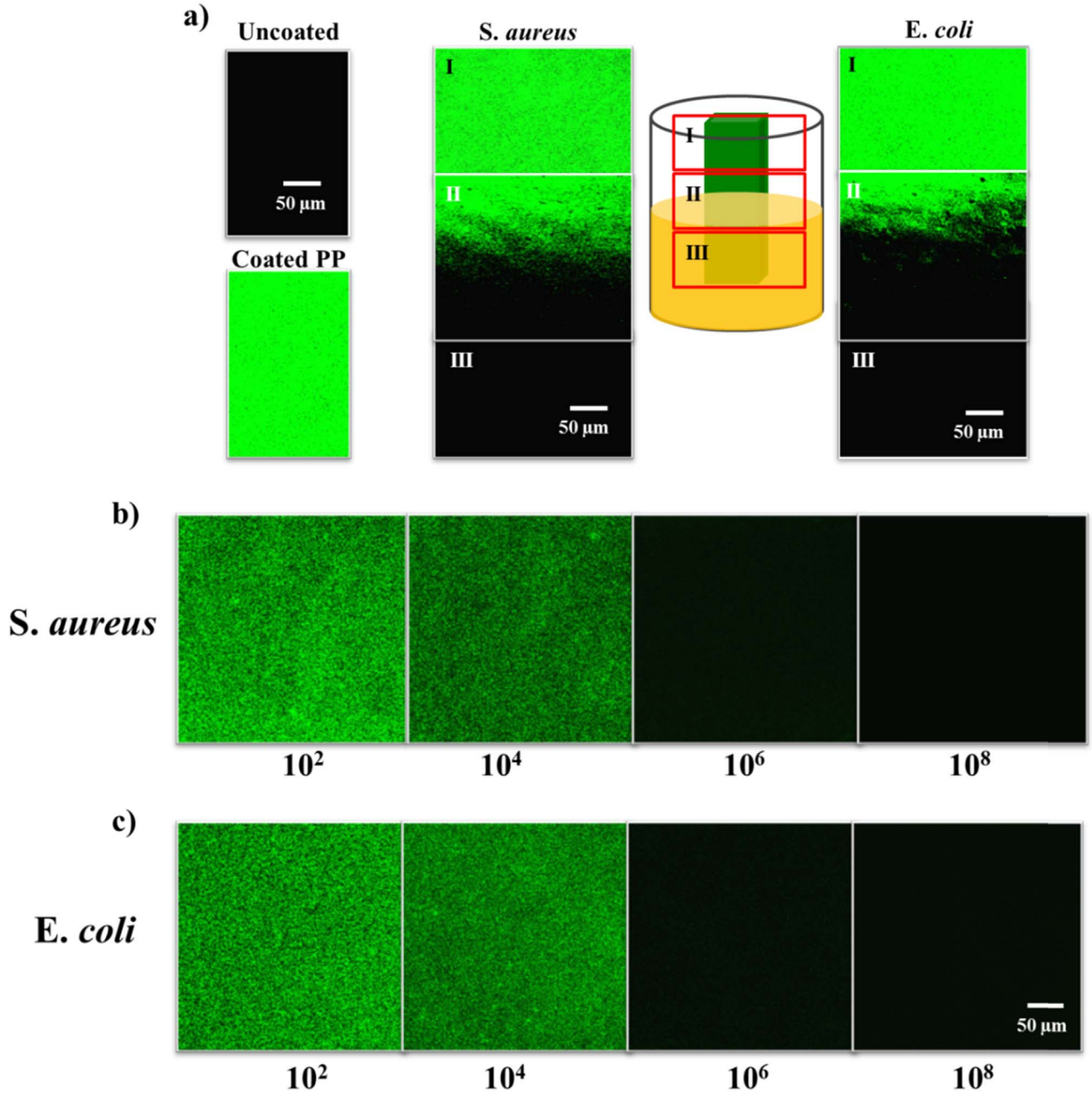

Fig. 3. Confocal laser scanning microscopy (CLSM) images of (a) uncoated PP, coated PP, PP coated with F-PVP after interaction with bacteria at the top (I) middle (II) and bottom (III) of the slide. PP coated with F-PVP after interaction with bacteria at different concentrations (CFU/mL) of (b) S. *aureus* (c) E. *coli*. The bacterial concentration was 10^8 CFU/mL and the concentration of F-PVP was 1 mg/mL. (For interpretation of the references to color in this figure, the reader is referred to the web version of this article.)

3.5. Evidences of PP film and bacteria interaction

SEM investigation, as shown in Fig. 4, demonstrated the adherence of both bacterial strains to the PP surface after incubation for 1 h, clearly showing that the polyion complex and hydrophobic interactions occurred between the bacteria and the cationic groups of F-PVP. Furthermore, we characterized how PP film, PP coated with F-PVP, and coated PP interact with bacteria by XPS analysis, to understanding the interactions between each element. Fig. 4b shows that C, O, N, and Br were identified by the wide-scan spectra, and only a C1s peak was observed in XPS analysis of PP film alone (Fig. S7). The results confirmed successful coating of the F-PVP on the PP film even though the peaks of B and F as elemental in BODIPY were not appear due to single unit of BODIPY in PVP backbone. Instead of XPS spectra, we verify BODIPY moieties using UV–vis spectroscopy and PL spectra, showing absorption peak at 550 nm and green emission when excited at 520 as BODIPY properties (Cheng et al., 2013; Kang et al., 2016). In the survey-scan spectrum of coated PP after interact with *E. coli* (Fig. 4c), a new peak of P was identified between 132 and 134 eV, confirming the presence of bacteria on the surface of the coated PP. Compared with *E. coli*, the peak of P in the XPS spectrum PP exposed to *S. aureus* (Fig. 4d**)** showed a lower intensity at the same binding energy region. This was concordant with the smaller quantity of phosphate groups in the cell wall of *S. aureus* than *E. coli* (Y.Q. Li et al., 2014; Y. Li et al., 2014), In the narrow-scan spectra, the peaks centered at 533 and 532 eV reflected the O 1s for all spectra. In all C 1 s XPS spectra, three peaks were observed at approximately 283.9, 285.8, and 287.9 eV, indicating C–C, C–N and C=O bonds, respectively. The peak of N 1s was confirmed at 399 eV, and the cationic amine (N1) and neutral amine (N°) peaks of N 1s were observed at 399.5 and 402.3 eV,

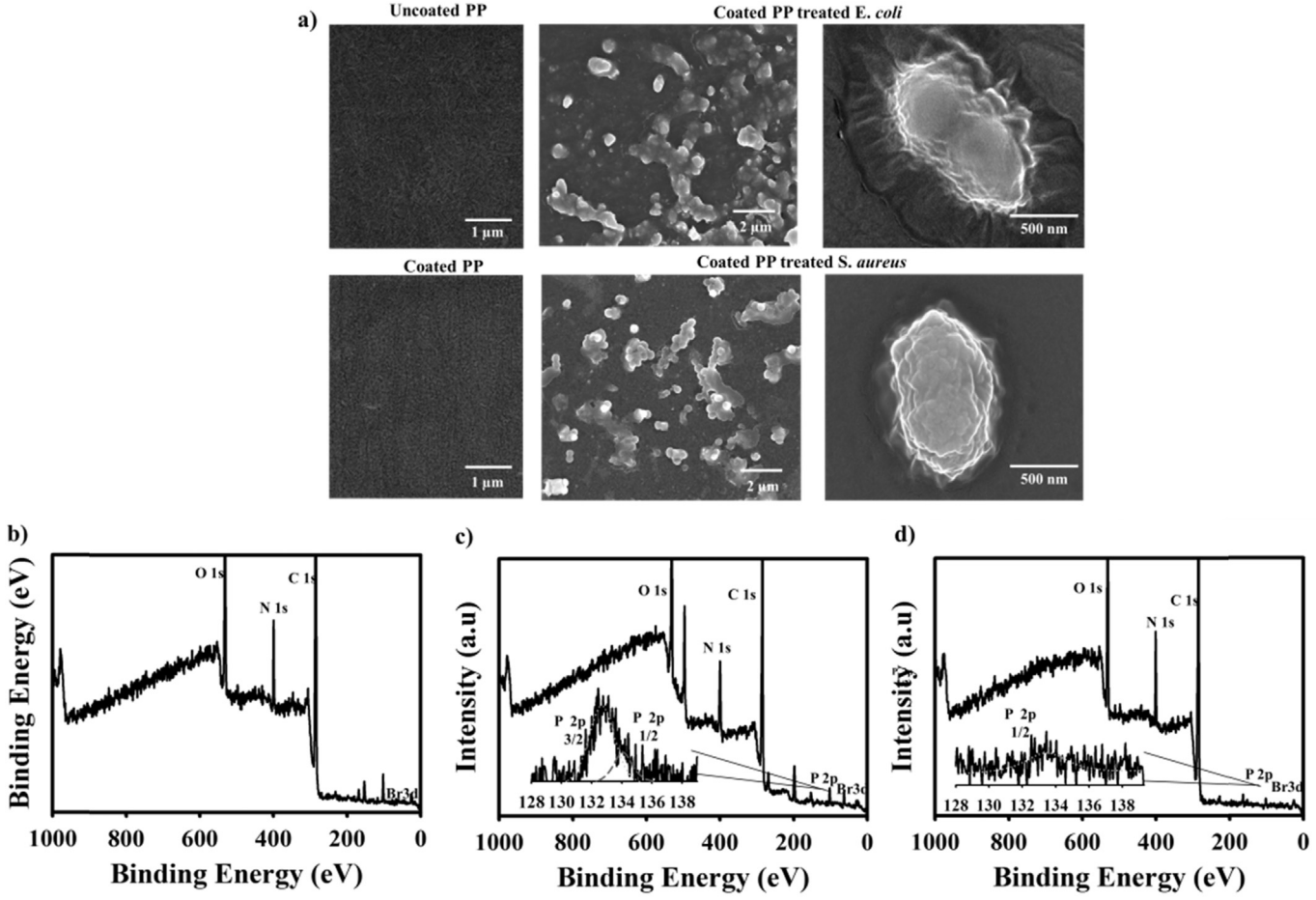

Fig. 4. SEM images of (a) uncoated PP and PP coated with F-PVP after interaction with *S. aureus* and *E coli*. The bacterial concentration was 10^8 CFU/mL and the concentration of F-PVP was 1 mg/mL. (b) XPS of PP coated with F-PVP (c) XPS of PP coated with F-PVP after interaction with *E. coli* and (d) *S. aureus*. The insert is an enlarged view of the P 2p spectra.

respectively (Fig. S7) (Jeong et al., 2015). The XPS analysis confirmed the successful of coating PP by F-PVP and the interaction between each element in the bacteria with the coated PP surface.

3.6. NIR-responsive F-PVP for photothermal killing

Since this platform contained NIR-responsive IR825 quaternized with the PVP backbone, we observed the capacity for thermal killing of bacteria using confocal live/dead and SEM images, the elevation appearance from 0.1 to 5 mg/mL of F-PVP mediated by NIR irradiation are shown in Fig. S4. Fig. 5a exhibit fluorescence labeling with SYTO 9 (green) for live cell and propidium iodide (red) for dead cell of bacteria treated F-PVP (Ghosh et al., 2014). Bacteria treated F-PVP and NIR irradiation showed many dead cells (red), whereas bacteria treated with the cationic polymer without NIR exposure showed many live cells (green), confirming that photothermal heating produced cell death of *S. aureus* and *E. coli*. Furthermore, the NIR-irradiated F-PVP killed bacterial cells, the cell bacteria deformed and aggregated as shown in Fig. 5b. The heat damage on cell bacteria was caused inactivation of many essential functions such as substance transport, ATP synthesis, and other cell maintenance processes, generated inhibition of recurring bacterial proliferation. Another previous study, the NIR induce heat release of the nanoporous gold disks arrays can kill three type bacteria including thermophilic bacteria (Greggy et al., 2016). It means our system can also produce photothermal destroyed by causing irreparable cellular bacteria damage even to heat resistance bacteria. We also observed the bacteria killing efficiency of F-PVP from 10^2 to 10^8 cells/mL towards S. *aureus* and E. *coli* using MTT assay. As a result shown in Fig. S5, the F-PVP under NIR irradiation can kill almost 100% of S. *aureus* and E. *coli* at different concentration of bacteria, indicating the killing effect towards both bacteria because of heat release induced NIR exposure of F-PVP. Comparing to bacteria treated F-PVP without NIR irradiation as a control, the cell bacteria still alive, implicating the F-PVP have no antibacterial activity without NIR exposure. However, this platform could be used for efficient photothermal killing of bacteria (Mazrad et al., 2016; Park et al., 2016).

4. Conclusion

We have firstly reported a combined polymer to obtain a cationic substituent for rapid and simple detection of gram-positive and gram-negative bacteria not only in aqueous but also in solid phase assay. The combined NIR-responsive IR825 and fluorescent BODIPY at PVP backbone revealed bacterial detection ability based on a fluorescent on/off system in the aqueous phase, as proved by SEM images showing the adherence polymer in surface bacteria. Our unique approach utilizes the catechol moieties as a coating agent for various substrates to produce a solid-phase assay with superior detection performance. The detection limit was 1 mg/mL for the liquid-phase assay and the minimal detectable concentration of bacteria using the solid-phase assay was 10^6 CFU/mL. This biosensor also exhibited good antibacterial activity induced by NIR irradiation by solution polymer but limited at coated PP. Finally, our approach can be used as biosensor to detect bacteria within simple and rapid detection in two ways, liquid and solid assay.

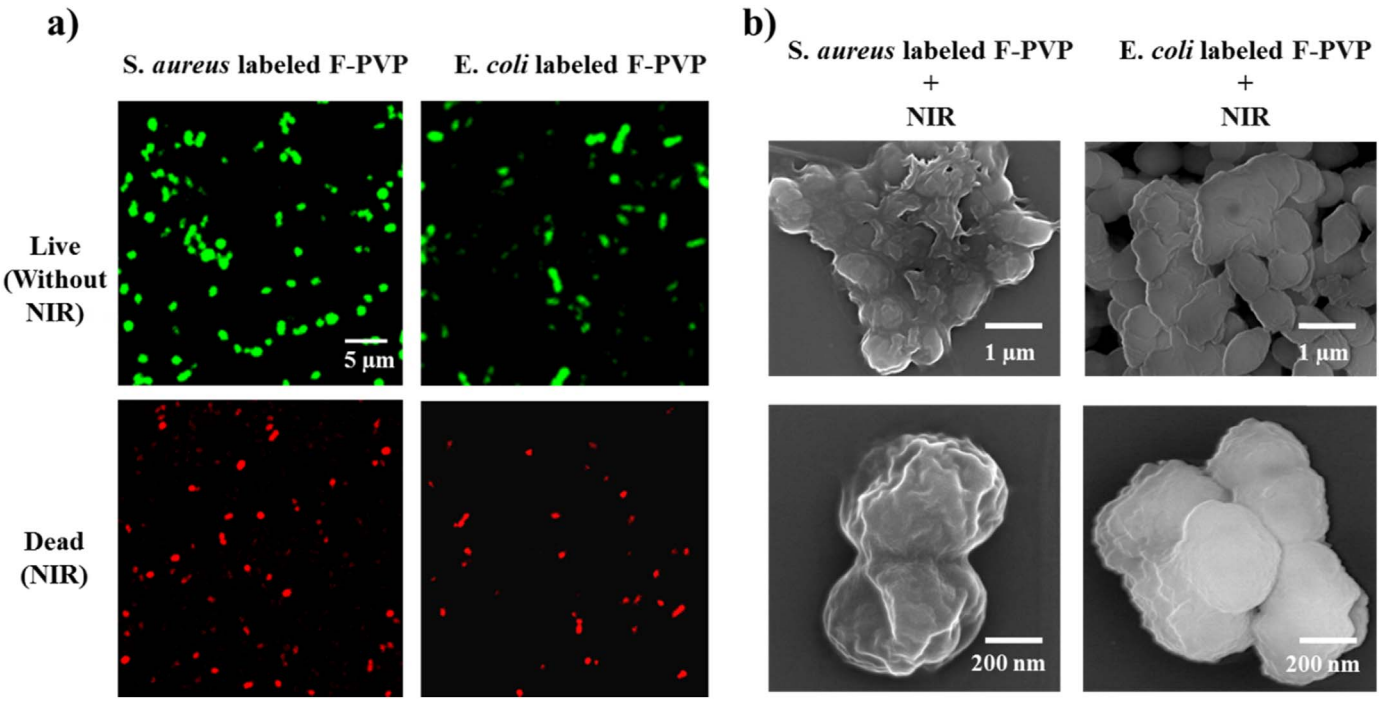

Fig. 5. Fluorescence microscopy images showing the PTT cytotoxicity of bacteria labeled with F-PVP after 5 min of 808-nm NIR irradiation in SYTO 9 and PI (scale=5 μm). (b) SEM images of bacteria labeled with F-PVP after 5 min 808 nm NIR irradiation at a concentration of 1 mg/mL. (For interpretation of the references to color in this figure, the reader is referred to the web version of this article.)

Author informations

S.Y.P., K.D.L., and I. I. supervised the project and Z. A. I. M. realized the all experiments and measurements.

Acknowledgements

This work was supported by the Grant No. 10048377, 10062079 and R0005237 from the Ministry of Trade, Industry & Energy (MOTIE), Fusion Research R & D Program from the Korea Research Council for Industrial Science & Technology (No. G02054), Basic Science Research Program through the National Research Foundation of Korea (NRF) funded by the Ministry of Education (No. 2014055946), and Marine Biotechnology Program (No. 20150220) funded by Ministry of Oceans and Fisheries, South Korea.

Appendix A. Supplementary material

Supplementary data associated with this article can be found in the online version at doi:10.1016/j.bios.2016.10.027.

References

Bandyopadhyay, A., McCarthy, K.A., Kelly, M.A., Gao, J., 2015. Nat. Commun., 6. http://dx.doi.org/10.1038/ncomms7561.
Birdsell, D.C., Doyle, R.J., Morgenstern, M., 1975. J. Bacteriol. 121, 726–734.
Chae, K.H., Baek, S.J., 2012. Macromol. Chem. Phys. 213, 1190–1195.
Chen, W., Li, Q., Zheng, W., Hu, F., Zhang, G., Wang, Z., Zhang, D., Jiang, X., 2014. Angew. Chem. 126, 13954–13959.
Cheng, L., He, W., Gong, H., Wang, C., Chen, Q., Cheng, Z., Liu, Z., 2013. Adv. Funct. Mater. 23, 5893–5902.
Cho, H.J., Chung, M., Shim, M.S., 2015. J. Ind. Eng. Chem. 31, 15–25.
Chung, H.J., Castro, C.M., Im, H., Lee, H., Weissleder, R., 2013. Nat. Nanotechnol. 8, 369–375.
Fauci, A.S., Morens, D.M., 2012. N. Engl. J. Med. 366, 454–461.
Fischer, E.R., Hansen, B.T., Nair, V., Hoyt, F.H., Dorward, D.W., 2012. Curr. Protoc. Microbiol. B 2, 1–76.
Gebert, S., Siegel, D., Wellinghausen, N., 2008. J. Infect. 57, 307–316.
Ghosh, C., Manjunath, G.B., Akkapeddi, P., Yarlagadda, V., Hoque, J., Uppu, D.S.S.M., Konai, M.M., Haldar, J., 2014. J. Med. Chem. 57, 1428–1436.
Goy, R.C., Morais, S.T.B., Assis, O.B.G., 2016. Rev. Bras. Farmacogn. 26, 122–127.
Greggy, M.S., Felipe, I.D.S.F., Fusheng, Z., Debora, F.E., Wei, C.S., 2016. Opt. Mater. Express 6, 1217–1229.
Jann, B., Reske, K., Jann, K., 1975. Eur. J. Biochem. 60, 239–246.
Jeong, C.J., Kang, E.B., Park, S.J., Choi, K.H., Shin, G., In, I., Park, S.Y., 2015. Polym. Eng. Sci.. http://dx.doi.org/10.1002/pen.
Kang, D.K., Ali, M.M., Zhang, K., Huang, S.S., Peterson, E., Digman, M.A., Gratton, E., Zhao, W., 2014. Nat. Commun., 5. http://dx.doi.org/10.1038/ncomms6427.
Kang, E.B., Lee, J.E., Jeong, J.H., Lee, G., In, I., Park, S.Y., 2016. J. Ind. Eng. Chem. 33, 336–344.
Khan, R., Islam, B., Akram, M., Shakil, S., Ahmad, A.A., Ali, S.M., Siddiqui, M., Khan, A.U., 2009. Molecules 14, 586–597.
Kim, Y.K., Sharker, S.M., In, I., Park, S.Y., 2016. Carbon 103, 412–420.
Lazcka, O.F., Campo, J.D., Muñoz, F.X., 2007. Biosens. Bioelectron. 22, 1205–1217.
Lee, H., Lee, Y., Statz, A.R., Rho, J., Park, T.G., Messersmith, P.B., 2008. Adv. Mater. 20, 1619–1623.
Lee, K.S., In, I., Park, S.Y., 2014. Appl. Surf. Sci. 313, 532–536.
Lee, S.Y., Kim, S.H., Kim, S.M., Lee, H., Lee, G., Park, S.Y., 2014. New J. Chem. 38, 2225–2228.
Li, Y., Hu, X., Tian, S., Li, Y., Zhang, G., Zhang, G., Liu, S., 2014. Biomaterials 35, 1618–1626.
Li, Y.Q., Zhu, B., Li, Y., Leow, W.R., Goh, R., Ma, B., Fong, E., Tang, M., Chen, X., 2014. Angew. Chem. Int. Ed. 53, 5837–5841.
Magin, C.M., Cooper, S.P., Brennan, A.B., 2010. Mater. Today 13, 36–44.
Mazrad, Z.A.I., In, I., Park, S.Y., 2016. RSC Adv. 6, 54486–54494.
Miranda, O.R., Li, X., Gonzalez, L.G., Zhu, Z.J., Yan, B., Bunz, U.H.F., Rotello, V.M., 2011. J. Am. Chem. Soc. 133, 9650–9653.
Ning, X., Lee, S., Wang, Z., Kim, D., Stubblefield, B., Gilbert, E., Murthy, N., 2011. Nat. Mater. 10, 602–607.
Park, S.J., Kang, E.B., Sharker, S.M., Lee, G., In, I., Park, S.Y., 2016. Macromol. Mater. Eng. 301, 141–148.
Ray, P.C., Khan, S.A., Singh, A.K., Senapati, D., Fan, Z., 2012. Chem. Soc. Rev. 41, 3193–3209.
Valloran, J.J., Handschin, S., Pillai, S.M., Vetter, B.N., Rusch, S., Beck, H.P., Mezzenga, R., 2016. Adv. Funct. Mater. 26, 181–190.
Wang, H., Zhou, Y., Jiang, X., Sun, B., Zhu, Y., Wang, H., Su, Y., He, Y., 2015. Angew. Chem. Int. Ed. 54, 5132–5136.
Wei, Q., Achazi, K., Liebe, H., Schulz, A., Noeske, P.L.M., Grunwald, I., Haag, R., 2014. Angew. Chem. Int. Ed. 53, 11650–11655.
Wilson, M.L., Weinstein, M.P., Mirrett, S., Reimer, L.G., Feldman, R.J., Chuard, C.R., Reller, L.B., 1995. J. Clin. Microbiol. 33, 2265–2270.
Wilson, W.W., Wade, M.M., Holman, S.C., Champlin, F.R., 2001. J. Microbiol. Methods 43, 153–164.
Yang, C., Xie, H., Li, Q.C., Sun, E.J., Su, B.L., 2015. J. Colloid Interface Sci. 450, 388–395.
Yeroslavsky, G., Girshevitz, O., Frey, J.F., Donovan, D.M., Rahimipour, S., 2015. Langmuir 31, 1064–1073.
Yuan, H., Liu, Z., Liu, L., Lv, F., Wang, Y., Wang, S., 2014. Adv. Mater. 26, 4333–43338.
Zhao, Y., Ye, M., Chao, Q., Jia, N., Ge, Y., Shen, H., 2009. J. Agric. Food Chem. 57, 517–524.